Investigation of fluorine octahedron connectivities in transition metal fluoride glasses by solid-state ^{19}F magic-angle-spinning nuclear magnetic resonance spectroscopy

1997 J. Phys.: Condens. Matter 9 6719

(http://iopscience.iop.org/0953-8984/9/31/022)

J. Phys.: Condens. Matter **9** (1997) 6719–6736. Printed in the UK PII: S0953-8984(97)82239-4

Investigation of fluorine octahedron connectivities in transition metal fluoride glasses by solid-state ^{19}F magic-angle-spinning nuclear magnetic resonance spectroscopy

B Bureau†§, G Silly†, J Y Buzaré†, J Emery†, C Legein‡ and C Jacoboni‡

† Laboratoire de Physique de l'Etat Condensé, UPRES-A CNRS No 6087, Université du Maine, Avenue Olivier Messiaen, 72085 Le Mans Cédex 9, France

‡ Laboratoire des Fluorures, UPRES-A CNRS No 6010, Université du Maine, Avenue Olivier Messiaen, 72085 Le Mans Cédex 9, France

Received 28 February 1997, in final form 22 May 1997

Abstract. High-resolution magic-angle-spinning (MAS) ^{19}F NMR spectroscopy is used to investigate the structural properties of some transition metal fluoride glasses (PbF_2–ZnF_2–GaF_3) related to the fluorine network. Several glass compositions are investigated in order to vary the $PbF_2/ZnF_2/GaF_3$ ratios. ^{19}F MAS NMR experiments are carried out on certain crystalline compounds selected as being the initial constituents (PbF_2, ZnF_2, GaF_3) or recrystallization compounds (Pb_2ZnF_6, $PbGaF_5$, $Pb_3Ga_2F_{12}$, $Pb_9Ga_2F_{24}$) of glassy phases, or because they have some specific particular connectivities of the fluorine octahedron network (e.g. $CsZnGaF_6$).

It is shown that three types of fluorine are involved in the glass network: free fluorines which are not connected to transition metal ions, and shared and unshared fluorines belonging to $(ZnF_6)^{4-}$ and $(GaF_6)^{3-}$ octahedra. Quantitative information on these three different fluorine sites, their relative ratios in the glassy networks, and the degree of cross-linking of the fluorine octahedra is obtained. Our results prove the validity of the previously adopted assumption according to which the glass network is built up from corner-sharing fluorine octahedra centred on transition metal ions.

1. Introduction

This paper contains a study of the structural properties of some transition metal fluoride glasses (PbF_2–ZnF_2–GaF_3) by NMR spectroscopy.

On the basis of the early studies [1–5], the TMFG networks are usually described as mixed packings of F^- ions and Pb^{2+} cations due to the closeness of their ionic radii, with the transition metal ions Zn^{2+} and Ga^{3+} in octahedral holes. It is also commonly assumed that the network of these glasses is built up of chains of fluorine corner-sharing octahedra, $(ZnF_6)^{4-}$ and $(GaF_6)^{3-}$, with Pb^{2+} ions at the interstitial sites.

In the past few years, EPR studies have been undertaken to investigate the octahedron network in these glasses more precisely [6–9]. The main conclusion obtained by this technique is that the octahedra are only slightly distorted, and, furthermore, distributions of the radial and angular distortions were given.

In the present work, we are mainly interested in investigating the connectivity between the octahedra, and estimating their degree of cross-linking. Owing to the specific role played

§ E-mail: bureau@lola.univ-lemans.fr.

0953-8984/97/316719+18$19.50

by the fluorine atoms in the structure, it appears that ^{19}F NMR should be well adapted to provide an answer to this question. Nevertheless, it is well known that the ^{19}F NMR spectra are poorly resolved in conventional experiments due to dipolar broadening and chemical shift anisotropy [10–12]. So, we used high-resolution magic-angle-spinning (MAS) ^{19}F NMR spectroscopy in order to reduce the line broadening.

As many structural features are claimed to be similar in the glasses and in the crystalline phases of close compositions, some ^{19}F MAS NMR experiments were carried out on selected crystalline compounds that are interesting because they are either the initial constituents (PbF_2, ZnF_2, GaF_3) or recrystallization compounds (Pb_2ZnF_6, $PbGaF_5$, $Pb_3Ga_2F_{12}$, $Pb_9Ga_2F_{24}$) of glassy phases, or because they have some specific particular connectivity of the fluorine octahedron network (e.g. $CsZnGaF_6$). Furthermore, several glass compositions were investigated in order to vary the $PbF_2/ZnF_2/GaF_3$ ratios.

It will be shown that such an approach allows us to find evidence for three types of fluorine: free fluorines which are not connected to transition metal ions, and shared and unshared fluorines belonging to $(ZnF_6)^{4-}$ and $(GaF_6)^{3-}$ octahedra. We obtain valuable information on the characterization of these three different fluorine sites, their relative contributions in the glassy networks, and the cross-linking of the fluorine octahedra.

2. Experimental procedure

PZG glasses were obtained using the following procedure: after preliminary mixing of the starting crystalline constituents PbF_2, ZnF_2, and GaF_3, the melt was placed in a covered platinum crucible, heated to 800 °C, and then quenched on a cold plate. No stabilizer, such as AlF_3 or YF_3, was added to our mixtures.

Crystalline compounds were obtained from solid-state reaction of a stoichiometric mixture, in sealed platinum tubes. The synthesis conditions are summarized in table 1. The crystallinity and the crystal structure of these compounds were controlled by x-ray experiments.

The ^{19}F NMR spectra were recorded at room temperature on an MSL 300 Bruker spectrometer operating at 282.282 MHz, with a BRUKER 4 mm MAS probe spinning at 15 kHz. The processing and acquisition parameters were: 7 to 9 μs single-$\pi/2$-pulse duration; 1 s recycle time; spectral width 300 kHz; time domain 1 K; and 100 or 200 scans per spectrum. The ^{19}F chemical shifts are given in ppm with respect to an external reference, C_6F_6.

3. ^{19}F NMR chemical shift measurements

3.1. Measurements on the PZG fluoride glass

This preliminary investigation was carried out on the PZG glass with the molar composition 40 PbF_2, 20 ZnF_2, 40 GaF_3. The ^{19}F MAS NMR spectra recorded at different rotation speeds are compared in figure 1. By increasing the spinning speed, we simultaneously average the chemical shift and reduce the strong dipolar interaction essentially due to F^- ions. Hence, a line narrowing occurs, and three different fluorine lines, a, b, and c, are evidenced at 157, 68.5, and 8.5 ppm, respectively. We distinguish the actual fluorine lines from the spinning side bands by the invariance of the line positions at all spin rates.

In order to determine the nature of the fluorine sites related to the a, b, and c lines, we decided to investigate the ^{19}F chemical shifts in crystalline compounds related to the glasses. In the following, we present the results obtained for the starting constituents

Table 1. Times, temperatures, and conditions of preparation for the crystalline compounds.

Compound	Time in furnace (hours)	Furnace temperature (°C)
β-PbF_2	18	400 + quenching
Pb_2ZnF_6	120	510
$CsZnGaF_6$	15	650 + quenching
$PbGaF_5$	24	630
$Pb_3Ga_2F_{12}$	24	520
$Pb_9Ga_2F_{24}$	24	520

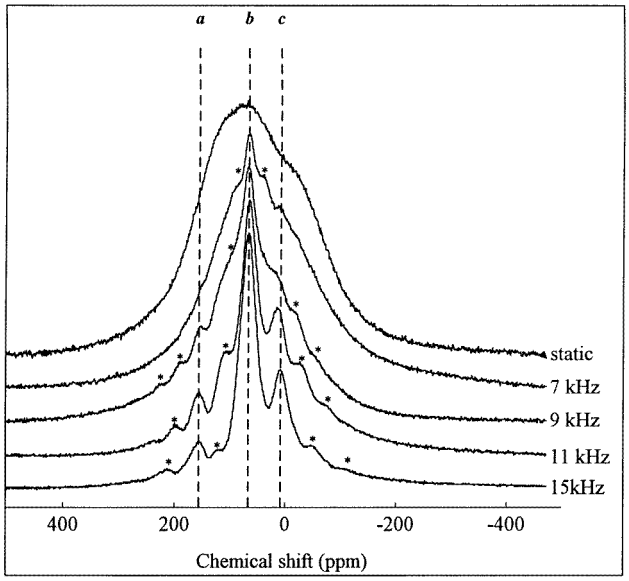

Figure 1. ^{19}F NMR spectra for PZG C glass at 0, 7, 9, 11, and 15 kHz spinning rates. The lines labelled $*$ are spinning side bands.

(PbF_2, ZnF_2, and GaF_3), and some crystalline phases containing Pb^{2+}, Ga^{3+}, and Zn^{2+} built up from fluorine octahedra with different connectivities. We pay a particular attention to the compounds resulting from the recrystallization of the glasses: $PbGaF_5$, $Pb_3Ga_2F_{12}$, $Pb_9Ga_2F_{24}$, and Pb_2ZnF_6 [8].

3.2. Measurements on the starting crystalline constituents

The MAS NMR spectra of the starting constituents, obtained at a spinning frequency of 15 kHz, are presented in the upper part of figure 2, just below the PZG glass spectrum. Despite the high spinning frequency, the lines remain broad due to the large dipolar couplings always involved in fluorine compounds.

3.2.1. α-PbF_2. This is the common stable phase of lead fluoride at room temperature. The line narrowing is sufficient for one to distinguish the two different ^{19}F NMR lines at 153 and 116 ppm and for one to observe a structure on the lines due to J-coupling between ^{19}F and ^{207}Pb nuclei, as previously mentioned [13]. The two different sites are in agreement

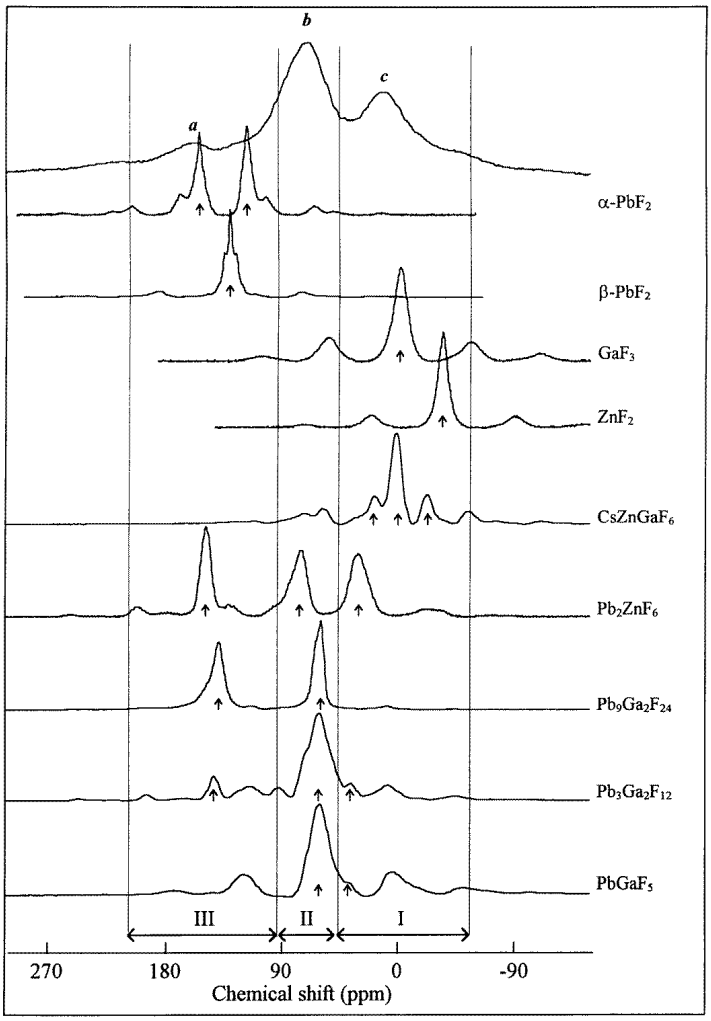

Figure 2. A comparison of the ^{19}F NMR spectra for PZG C glass, the starting constituents, $CsZnGaF_6$, and the recrystallization compounds. The arrows denote the central lines for each site.

with the crystallographic data: α-PbF_2 is orthorhombic with the space group *Pnma* [14]. In this case, there exist two different sites for the F^- ion. The first one, for the fluorine ions labelled F(1), with local symmetry *m*, corresponds to fluorine ions at the centre of distorted tetrahedra with an average bond length equal to 2.52 Å. In the second one, the fluorine ions labelled F(2) with local symmetry *m* too, are coordinated to five Pb^{2+} ions with a mean Pb^{2+}–F^- distance equal to 2.77 Å. The NMR lines at 153 ppm and 116 ppm may be attributed to F(1) and F(2) fluorines respectively [13].

3.2.2. β-PbF_2. This is the PbF_2 high-temperature ($T > 18$ °C) phase of cubic fluorite type, obtained by quenching at 400 °C. The only NMR line for β-PbF_2 at 129 ppm is also consistent with the crystallographic data: an $Fm3m$ space group with cell parameter

$a = 5.9273$ Å [15]. Each F^- ion is at the centre of a Pb^{2+}-ion regular tetrahedron; the local symmetry is $\bar{4}3m$. All of the fluorines are equivalent, with the F^-–Pb^{2+} distance equal to $a\sqrt{3}/4 = 2.5666$ Å. The fluorine-ion network is built up from F^- cubes. The ^{19}F isotropic chemical shift in β-PbF_2 is intermediate between the values obtained for the two sites in α-PbF_2, in agreement with an intermediate Pb^{2+}–F^- bond length. It may be the case that the J-coupling structure in β-PbF_2 is better resolved than in α-PbF_2, due to the more regular environment of the F^- ions.

3.2.3. GaF_3. The ^{19}F NMR spectrum of GaF_3 consists of one line at -3 ppm indicating a unique ^{19}F site in this compound. In fact, GaF_3 crystal is rhombohedral, with space group $R\bar{3}c$; the hexagonal cell parameters are $a = 5.002$ Å and $c = 12.973$ Å. All of the fluorine ions are equivalent, with local symmetry 2. The network is built up from corner-sharing $(GaF_6)^{3-}$ octahedra [16]. Hence, in this situation, each of the fluorines is shared between two different octahedra.

3.2.4. ZnF_2. ZnF_2 has a rutile structure, like CoF_2, MnF_2 and MgF_2 [15, 17]. The space group symmetry is $P4_2/mnm$, with cell parameters $a = 4.7034$ Å and $c = 3.3670$ Å. All of the fluorine ions are equivalent, but with two different Zn–F distances. The local symmetry is $m2m$. The network is built up of chains of edge-sharing octahedra linked together by corners. Each fluorine ion belongs to three distinct octahedra. As expected, the NMR spectrum exhibits only one line at -36.5 ppm connected to the equivalent ^{19}F nuclei.

From these first results, it may be seen that the positions of the lines are very sensitive to the environment of the fluorine ions. However, as shown in the upper part of the figure 2, there is not a full correspondence between the chemical shifts of the glass ^{19}F sites and those of the starting crystalline constituents. For instance, the b line is particular to the glass; the corresponding fluorine environment should be very different from those met in the basic compounds, as none of them exhibits any NMR line in the same chemical shift range.

3.3. Measurements on $CsZnGaF_6$

$CsZnGaF_6$ belongs to the pyrochlore family. As in GaF_3, each of the fluorines atoms is shared between two octahedra [18]. However, the Ga^{3+} and Zn^{2+} ions are statistically distributed among the centres of the octahedra, so there are three different types of neighbourhood for the fluorine nuclei: 25% of the fluorine ions are linked to two Zn^{2+} ions, 25% to two Ga^{3+} ions, and 50% to Zn^{2+} and Ga^{3+} ions.

The ^{19}F NMR spectrum of $CsZnGaF_6$ (figure 2) gives us a fair account of the situation: the inner line at -2.5 ppm is twice as intense as the two outer ones at -23.5 and 16 ppm respectively. Thus, the -2.5 ppm line is related to the Ga^{3+}–F^-–Zn^{2+} environment unambiguously. We may attribute the low-chemical-shift line to a Zn^{2+}–F^-–Zn^{2+} site, because the ^{19}F chemical shift is lower in ZnF_2 than in GaF_3. Moreover, the spin–spin relaxation time of the line at -23.5 ppm is longer ($T_2 = 159$ ms) than the one of the line at 16 ppm ($T_2 = 65$ ms), which is consistent with a spin–spin relaxation due to dipolar coupling: the more Ga^{3+} ions there are near a fluorine, the shorter the relaxation time should be (100% of Ga^{3+} ions have a nuclear spin, and only 4% of Zn^{2+} ions have one). Finally, the line at 16 ppm is attributed to Ga^{3+}–F^-–Ga^{3+} fluorines.

The mean position of the three lines at -3.3 ppm has to be compared with the GaF_3 line, which corresponds to corner-sharing fluorine octahedra. The positions of the three lines for $CsZnGaF_6$ allow us to infer that the c line observed for the glass has to be related to

shared F^- ions. However, it is not possible to differentiate the three possible environments under the c line of the glass, because of the remaining dipolar interaction and the distributed neighbourhood due to the glass structure.

Table 2. Numbers and types of neighbours and next-nearest neighbours for each fluorine crystallographic site in the Ba_2ZnF_6 structure.

$F^-(1)$	$F^-(2)$	$F^-(3)$
4 Ba^{2+} (2.607 Å)	2 Zn^{2+} (2.05 Å)	1 Zn^{2+} (1.968 Å)
8 F^- (2.9 and 2.934 Å)	8 F^- (2.842 and 2.9 Å)	8 F^- (2.842 and 2.934 Å)
		4 Ba^{2+} (2.941 Å)

3.4. Measurements on the PZG glass recrystallization compounds

3.4.1. Pb_2ZnF_6. The structure of Pb_2ZnF_6 has never been determined, but its x-ray diagram [19] is very close to those of Ba_2ZnF_6 and Ba_2NiF_6. Just some small extra lines appear, reflecting a slight symmetry lowering due to the Pb^{2+} ion. Nevertheless, it may be assumed that the structures of these compounds are similar. According to [20], the Ba_2ZnF_6 space group symmetry is $I\bar{4}22$, resulting in three distinct fluorine sites, $F^-(1)$, $F^-(2)$, and $F^-(3)$. The neighbourhood of each fluorine site is indicated in table 2. In Pb_2ZnF_6, the Pb^{2+} ion would take the place of the Ba^{2+} ion, and the Pb^{2+}–$F^-(1)$ bond length should be slightly shorter as the Pb^{2+} ion has a smaller ionic radius. The $F^-(1)$ site is then very similar to the $F^-(1)$ fluorine coordinated to four Pb^{2+} ions in α-PbF_2 [13, 14]. The $F^-(2)$ environment corresponds a F^- ion shared between two octahedra. In the $F^-(3)$ site, F^- ions belong to one octahedron. They will be called unshared F^- ions.

The Pb_2ZnF_6 NMR spectrum (figure 2) provides evidence of these three distinct environments. At 147 ppm, we can recognize the α-PbF_2-like line related to the fourfold-Pb^{2+}-coordinated fluorine ions. Therefore, the a line in the glass spectrum may be attributed to fluorines not connected to transition metal ions, with Pb^{2+} ions as nearest neighbours. We will call them free F^- ions in the following.

From the results obtained on $CsZnGaF_6$, we are able to distinguish the F(2) shared-fluorine line from the unshared-F(3) one for Pb_2ZnF_6. The line at 29.5 ppm for Pb_2ZnF_6 is close to the inner line at 16 ppm for $CsZnGaF_6$, and thus it may be related to the F(2) site of the former compound. Finally, we may infer that the line at 74 ppm corresponds to the F(3) site.

3.4.2. $PbGaF_5$, $Pb_3Ga_2F_{12}$, and $Pb_9Ga_2F_{24}$. $PbGaF_5$, $Pb_3Ga_2F_{12}$, and $Pb_9Ga_2F_{24}$ are interesting crystalline phases because they permit one to study the evolution of the spectra when, on the one hand, the number of Pb^{2+} ions for one fluorine increases from 1:5 to 3:8, and, on the other hand, the ratio Ga^{3+}/F^- decreases from 1:5 to 1:12. The results of the NMR spectra simulations, gathered together in table 3, show three kinds of line: at around 140 ppm, 60 ppm, and 35–40 ppm.

The first ones, at 140 ppm, correspond to the β-PbF_2-like line at 129 ppm: we attribute them to free F^- ions. As one would expect, the intensity of this line increases with the ratio Pb^{2+}/F^-. In the $PbGaF_5$ spectrum, the line completely vanishes: each of the F^- ions is connected to at least one transition metal ion.

The second lines, at 60 ppm, are close to the line at 74 ppm for Pb_2ZnF_6 attributed to unshared fluorines. In the $Pb_9Ga_2F_{24}$ spectrum, the total intensity is equally shared between

Table 3. Parameters of the ^{19}F NMR spectrum reconstruction of $PbGaF_5$, $Pb_3Ga_2F_{12}$, and $Pb_9Ga_2F_{24}$

Compounds		$PbGaF_5$	$Pb_3Ga_2F_{12}$	$Pb_9Ga_2F_{24}$
Ratio Pb^{2+}/F^-		1:5	1:4	3:8
Ratio Ga^{3+}/F^-		1:5	1:6	1:12
Isotropic	a-type line	—	141	139
chemical shift	b-type line	60	60	59
(ppm with respect to C_6F_6)	c-type line	40	34	—
Integrated	a-type line	0	13	50
intensities	b-type line	90	80	50
(%)	c-type line	10	7	0

this line and the one at 139 ppm. Hence, NMR suggests that the network of $Pb_9F_{12}(GaF_6)_2$ is built up of disconnected octahedra, and all of the fluorines belonging to the GaF_6 octahedra have to be classified as unshared F^- ions. So, we have definitely associated the 60 ppm lines with unshared F^- ions in $Pb_9Ga_2F_{24}$ and also in $Pb_3Ga_2F_{12}$ and $PbGaF_5$, where this kind of fluorine is expected to be in the majority.

The third lines, at around 35–40 ppm, may be attributed to shared F^- ions because, as already shown, their environment is quite different from that of the unshared fluorines (in particular, there is no Pb^{2+} ion among the nearest neighbours). Moreover, there is no such line in the $Pb_9Ga_2F_{24}$ spectrum, which is expected to have a structure with no shared F^- ions. Finally, the higher the ratio Ga^{3+}/F^-, the stronger the shared-F^- line intensity is.

The crystallographic structures of $PbGaF_5$ and $Pb_3Ga_2F_{12}$ have never been well established. Nevertheless, the structures of several compounds of this family ($(1-x)PbF_2$–xMF_3, with $M = Ga^{3+}$ or Fe^{3+}) have been correlated with that of $BaFeF_5$ [21]. According to [22], this compound is a good model for $PbGaF_5$. $BaFeF_5$ is composed of linear chains of fluorine octahedra and of chains of ramified fluorine octahedra [23], which leads to 20% shared and 80% unshared F^- ions. Recently, it was proposed that $BaTiF_5$ [24], rather than $BaFeF_5$, could be used to explain the $PbGaF_5$ structure. $BaTiF_5$ is composed of chains of ramified fluorine octahedra and of fluorine bioctahedra [25]. It gives 15% corner-sharing fluorine, 5% edge-sharing fluorine, and 80% unshared fluorine. In either case, the experimental intensities of the shared-fluorine lines in the $PbGaF_5$ spectrum are not in full agreement with the above results.

Furthermore, it may be stated that, in the $PbGaF_5$ and $Pb_3Ga_2F_{12}$ spectra, the main line, at 60 ppm, associated with the unshared fluorines, is much broader than in the $Pb_9Ga_2F_{24}$ spectrum. It may be seen as the superimposition of several components, arising because there are several slightly different environments. This is in agreement with the strong degree of disorder observed in these compounds, which may be correlated with the easiness of obtaining glasses of related compositions—which is not the case for $Pb_9Ga_2F_{24}$.

3.5. Measurements on the three types of fluorine ion in the PZG network

To sum up, the study of these fluoride crystalline phases enables us to divide the ^{19}F chemical shift scale into three distinct parts (figure 2):

(i) from -50 to 45 ppm (region I in figure 2), the lines correspond to F^- ions shared between two fluorine octahedra centred on transition metal ions;

(ii) from 50 to 90 ppm (region II), the lines correspond to unshared F^- ions belonging to fluorine octahedra centred on transition metal ions;

(iii) above 100 ppm (region III), the lines may be associated with free F^- ions with Pb^{2+} ions as nearest neighbours.

Each of the three lines of the PZG glasses belongs to one of these different zones represented in figure 2, and may now be easily classified: the a line corresponds to the free-fluorine site, the b line to the unshared-fluorine site, and the c line to the shared-fluorine site.

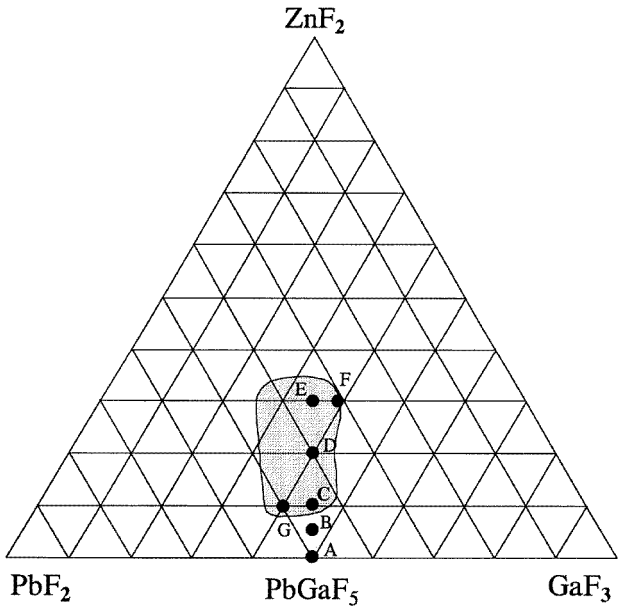

Figure 3. Localization of the seven PZG glasses labelled A to G in the area of glass formation in the ZnF_2–PbF_2–GaF_3 system.

4. Structural informations concerning the TMFG network

In order to obtain further results related to the way in which the octahedra are connected in these glasses, seven PZG glasses with different compositions were synthesized. In the area of PZG glass formation presented in figure 3 [26], the ZnF_2 percentage may be varied over a wide range, which permits one to synthesize several compositions (table 4). Two of them, A and B, are out of the area: we succeeded in synthesizing them because we did not have to worry about the thickness of the samples. We use just a cold plate (at around 20 °C) and a roller to quench the mixtures, instead of a mould as is usual, which corresponds to a cooling rate of about 400 °C s^{-1}.

All of the spectra were deconvoluted using the following procedure, which is illustrated in figure 4:

(i) the three lines are identified, as already described, using the invariance of their positions at different spinning rates;

Table 4. Compositions of the melt for the preparation of the seven PZG glasses.

Compounds	A	B	C	D	E	F	G
ZnF_2 (%)	0	5	10	20	30	30	10
GaF_3 (%)	50	47.5	45	40	35	38	40
PbF_2 (%)	50	47.5	45	40	35	32	50
Ratio Pb^{2+}/F^-	0.2	0.1919	0.1837	0.1667	0.1489	0.1345	0.2083

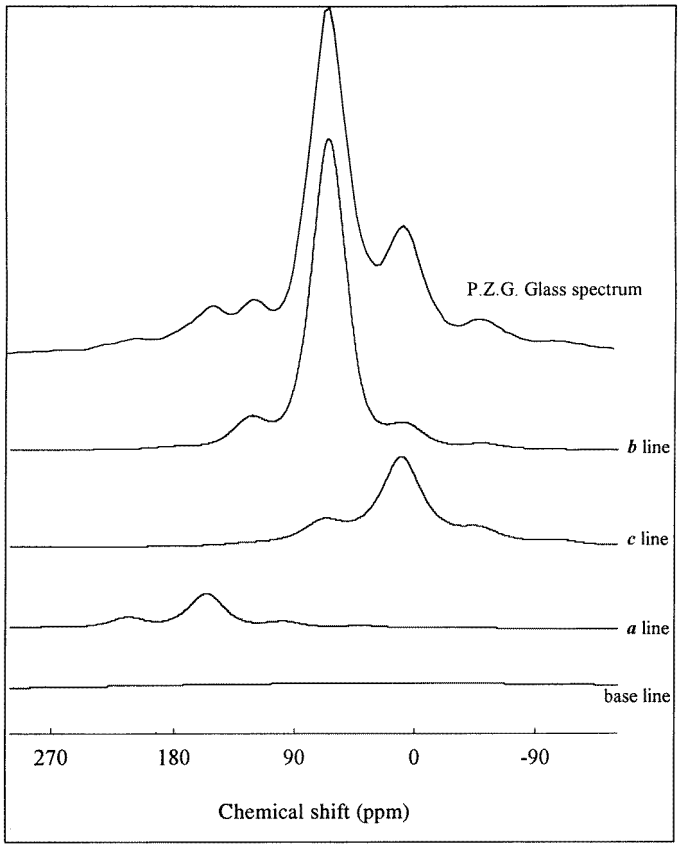

Figure 4. A reconstruction of ^{19}F MAS (15 kHz) NMR spectrum in PZG, showing evidence of the three different fluorine species.

(ii) a model of an anisotropic chemical shift enables us to fit the spinning side bands, using an extended version of Bruker Winfit Software [27];

(iii) it was necessary to introduce a broad Gaussian line to describe the base-line of the spectra which, as usually happens with ^{19}F spectra, is not flat because of the dead time.

The simulated and experimental lineshapes for the PZG glasses A, B, C, D, and E are compared in figure 5. All of the results are collected together in table 5. The integrated intensities were obtained after removing the contribution of the broad Gaussian line.

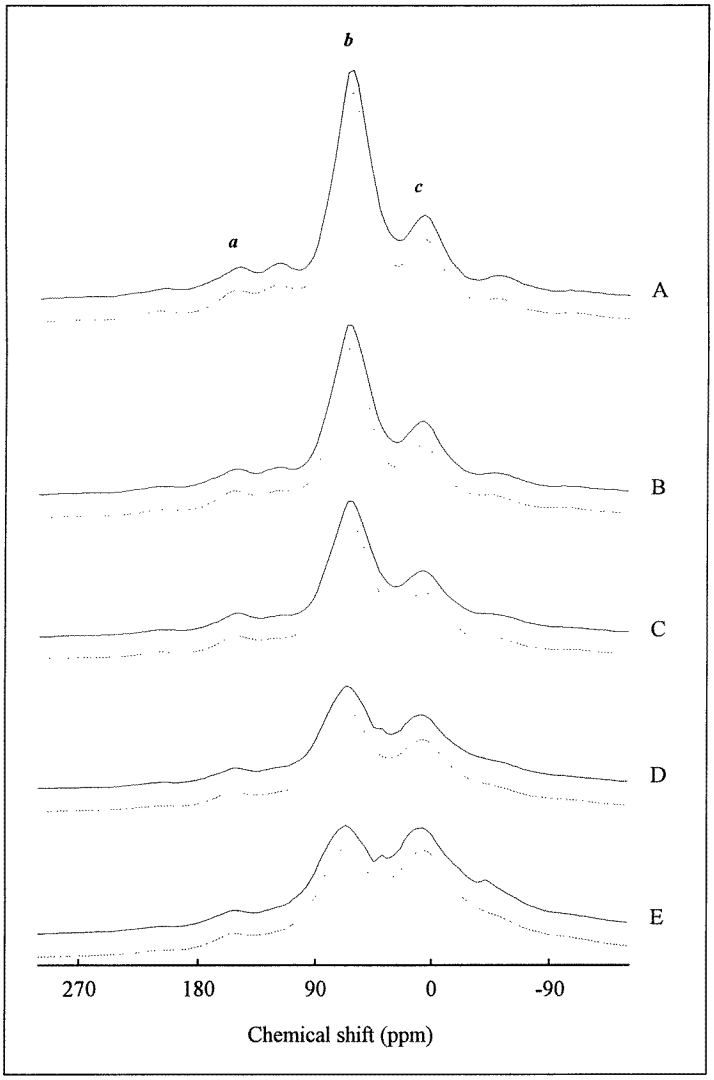

Figure 5. Simulated (dotted lines) and experimental (full lines) ^{19}F NMR spectra for PZG A, B, C, D, and E.

Through the evolution of the NMR spectra presented in figure 5, no tremendous variation of the a line can be observed. The main result is that the relative intensity of the c line increases with the ZnF_2 ratio to the detriment of the b line. This is in accordance with the previous interpretation of these lines: the number of octahedra increases while the number of fluorines decreases, so the shared-fluorine percentage can only grow.

It may be noted that the PZG A glass corresponds to the $PbGaF_5$ formula. The presence of free F^- ions in this glass is obvious, and the splitting between shared- and unshared-fluorine lines is clearly evident. This NMR spectrum, compared to the corresponding one obtained for the crystalline phase, mirrors the strong differences between the glass- and crystalline-phase networks.

Table 5. Parameters used for the reconstruction of the ^{19}F NMR spectra of the PZG glasses.

Glass composition		Line	A	B	C	D	E	F	G
Isotropic	±1 ppm	a	156	156	156	157	157	158	155
chemical shift		b	65	65.5	66	68.5	72	74	66.5
(ppm with respect to C_6F_6)		c	10	9.5	9	8.5	8	6	11
Widths (kHz)	±10%	a	8.8	8.8	8.5	8.5	8.8	8.5	8.2
		b	8.5	9.2	11.9	10.5	11.3	9.9	9.6
		c	10.5	11.0	10.2	14.7	16.4	15.8	13.0
Chemical shift	±10%	a	−105	−91	−94	−85	−85	−80	−85
anisotropy $[\sigma_{\parallel} - \sigma_{\perp}]$		b	−64	−57	−53	−51	−51	−80	−45
		c	−99	−96	−105	−96	−96	−90	−85
Gaussian/Lorentzian	±0.1	a	0.3	0.3	0.3	0.3	0.3	0.3	0.3
		b	0.5	0.5	0.5	0.5	0.5	0.5	0.5
		c	0	0	0	0	0	0	0
Integrated intensities	±3	a	10	9	8	6	5	3	11
(%)	±10	b	59	54	48	34	23	20	53
	±10	c	31	37	44	60	72	77	36

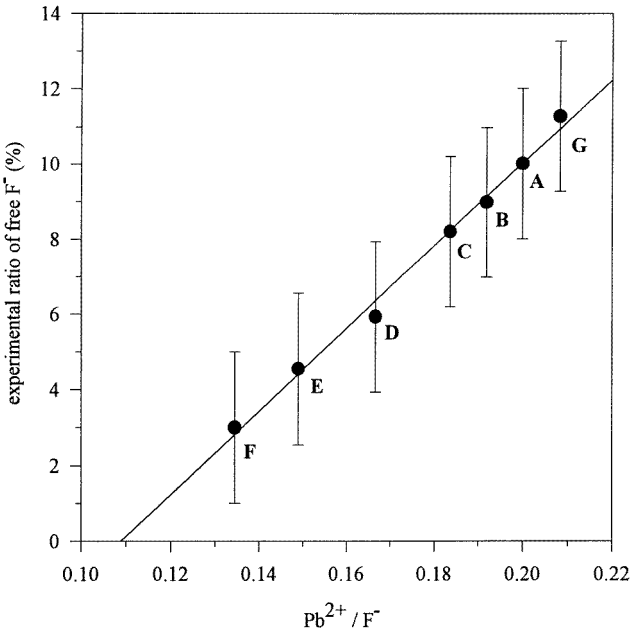

Figure 6. The experimental determination of the free-F^- ratio.

4.1. Determination of the number of free fluorines

From the previous results, it is thus possible to determine the ratios of free F^- ions in the different glasses, which is proportional to the relative intensity I_f of the a line in the NMR spectra. The results obtained for the $PbGaF_5$, $Pb_3Ga_2F_{12}$, and $Pb_9Ga_2F_{24}$ crystalline

compounds suggest that the number of free fluorines is closely related to the number of Pb^{2+} ions present in the glass. In figure 6, we present the relative intensity I_f of the a line versus r, the ratio of the number $n_{Pb^{2+}}$ of Pb^{2+} ions to the total number n of fluorines. The plot can be fitted by a linear law:

$$I_r = 110r - 12$$

with

$$r = \frac{n_{Pb^{2+}}}{n}.$$

This relation is in agreement with the fact that it is necessary to introduce a minimal quantity of PbF_2 into the melt for the a line to appear. Then, for $r < 0.11$, no free fluorine is present. The presence of at least four Pb^{2+} ions is needed to form the environment of a free fluorine.

To our knowledge, this is the first direct measurement of the free-fluorine ratio for these PZG glasses. This result should allow us to relate the shared- and unshared-F^- ratios deduced from integrated NMR line intensities to those deduced from the composition of the glass.

4.2. Identification and quantification of the other sites

From this result, and assuming as in the previous studies [1–3] that each transition metal ion (Ga^{3+} or Zn^{2+}) is surrounded by one fluorine octahedron, and that these octahedra could only be corner-sharing ones, it is then possible to determine the ratio of unshared (and shared) fluorines in the various glasses.

Table 6. Octahedron connection parameters and the fluorine ratios τ_f, τ_u, τ_s for the seven PZG glasses studied.

Glass composition		A	B	C	D	E	F	G
$(n - n_f)/n_o$		4.5	4.29	4.09	3.75	3.46	3.4	4.28
n_s/n_o		3	3.43	3.82	4.51	5.09	5.2	3.45
Fluorine ratio (%)	τ_f	10	9.1	8.2	6.3	4.4	2.8	10.9
	τ_u	60	54.5	48.9	37.4	25.3	22.9	53.2
	τ_s	30	36.4	42.9	56.3	70.3	74.3	35.9

In the following formula, n_u represents the number of unshared fluorines, n_f the number of free fluorines, n_s the number of shared fluorines, n the total number of fluorines, and n_o the total number of octahedra. The unshared fluorine ions belong to one octahedron, whereas the shared fluorines belong to two octahedra. Then, we can write

$$n = n_f + n_u + n_s \qquad \text{and} \qquad 6n_o = n_u + 2n_s$$

$$n = n_f + n_u + \left(\frac{6n_o - n_u}{2}\right)$$

or, with $\tau_u = 100n_u/n$,

$$\tau_u = 100\left(2 - 6\frac{n_o}{n}\right) - 2\tau_f.$$

n and n_o are known from the nominal composition of the glasses, and τ_f, which is equal to I_f, can be determined from the NMR spectrum simulation. It is then possible to calculate τ_u and $\tau_s = 100n_s/n$, where n_s represents the number of shared fluorines (table 6).

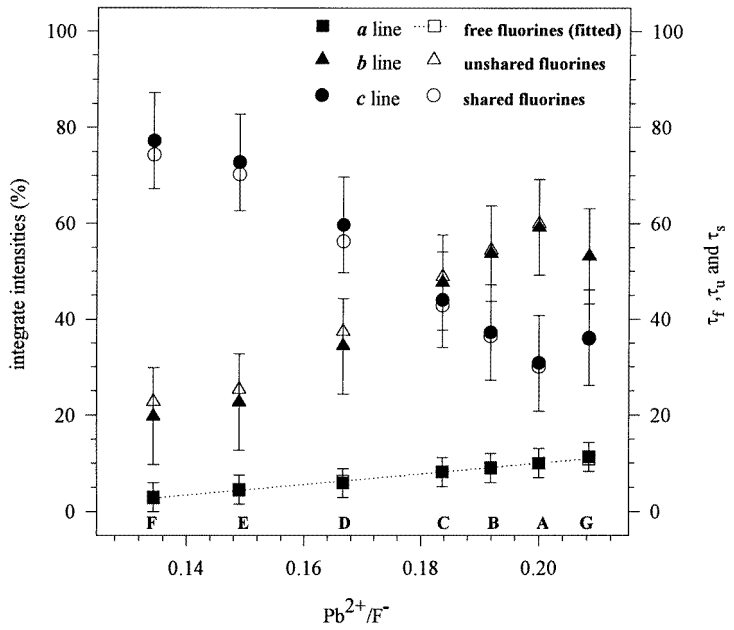

Figure 7. A comparison between the NMR a-, b-, and c-line normalized intensities and the free-, unshared-, and shared-fluorine ratios for the seven PZG glasses.

In figure 7, for each kind of fluorine, the relative intensities of the NMR b and c lines deduced from spectrum simulations are compared to the values of τ_u and τ_s obtained from the above equations. The agreement is fairly good. This confirms unambiguously that the octahedra are all corner-sharing ones, and that the b and c NMR lines correspond to unshared and shared fluorines respectively.

Additional information can be deduced from the NMR experiment. At this stage, the proportion of each kind of fluorine is known unambiguously. In the following, we will discuss the way in which the chains are connected to form the network of the glasses, in relation with their composition. Further comments will be made on the behaviour of the NMR parameters (linewidth, isotropic chemical shift, ...) obtained from the reconstruction of the spectra.

4.3. About the connections between fluorine octahedra

Two equivalent parameters can be used to obtain a quantitative view of the connection between the octahedra. The first one, and the one more commonly met in the literature, is the mean number of fluorines per octahedron, calculated as $(n - n_f)/n_o$. The second one, more useful to the visualization of the network, is the mean number of shared fluorines per octahedron, calculated as n_s/n_o (that is to say, the mean number of octahedra connected to one octahedron). These parameters are gathered together in table 6 for each of the different glass compositions. These values are to be compared with the four following interesting situations:

(i) the octahedra are isolated, as expected for $Pb_9Ga_2F_{24}$; then $(n - n_f)/n_o = 6$ and $n_s/n_o = 0$;

(ii) the octahedra are 1D connected to form isolated chains; then $(n - n_f)/n_o = 5$ and

$n_s/n_o = 2$;

(iii) the octahedra are 2D connected to form isolated planes, like in $RbAlF_4$; then $(n - n_f)/n_o = 4$ and $n_s/n_o = 4$;

(iv) the octahedra are built up into a 3D network, like in GaF_3; then $(n - n_f)/n_o = 3$ and $n_s/n_o = 6$.

So the seven glasses can be classified in two categories: the PZG A, B, C, and G glasses with 1D and 2D intermediate networks, and the PZG D, E, and F glasses with 2D and 3D intermediate networks. Thus we may infer that, in many cases, the chains of octahedra, in the usual description of the PZG glasses, intersect very often, and consequently only few octahedra belong to only one chain. Moreover, the above results show that it is possible to choose a given degree of cross-linking between the chains of octahedra by monitoring the glass composition.

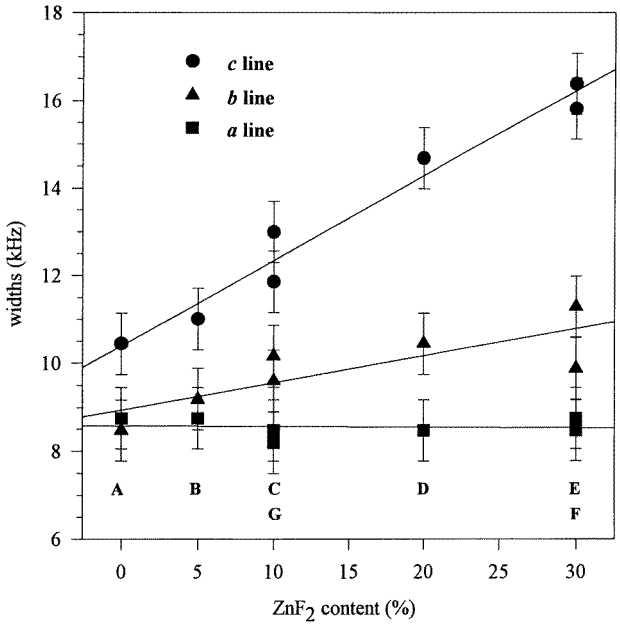

Figure 8. The ^{19}F NMR linewidth of the a, b, and c lines versus the ZnF_2 content in the starting melt.

4.4. Evolution of spectrum parameters with the glass composition

4.4.1. Linewidth behaviour. In figure 8, we present the evolution of the linewidth, for the three sites, versus the amount of ZnF_2 in the melt.

(i) For the c line, the strong increase of the linewidth is in accordance with the assignment of this line to shared fluorines. When the number of Zn^{2+} ions is equal to zero (PZG A = amorphous $PbGaF_5$), each fluorine ion is connected to two Ga^{3+} ions, which corresponds to the left-hand line of the ^{19}F NMR spectrum of $CsZnGaF_6$. When the number of Zn^{2+} ions in the melt increases, the three types of shared fluorine observed in $CsZnGaF_6$ contribute to the NMR spectrum. Thus, the higher the Zn^{2+} ratio in the melt, the higher the intensity of the line corresponding to the F^- ions connected to two Zn^{2+}

ions, which appears on the right-hand side of the c line. This phenomenon, added to the normal distribution of the sites in a glass, results in an increase of the width of this line.

(ii) For the b line, the effect is similar. The unshared fluorines are bonded to one transition metal ion which is either a Zn^{2+} or a Ga^{3+} ion. In this case too, the increase in the amount of ZnF_2 may result in a broadening of the line.

(iii) For the a line, no evolution is observed, as expected: the corresponding fluorines have Pb^{2+} ions as nearest neighbours. They are not really sensitive to the numbers of Zn^{2+} or Ga^{3+} ions.

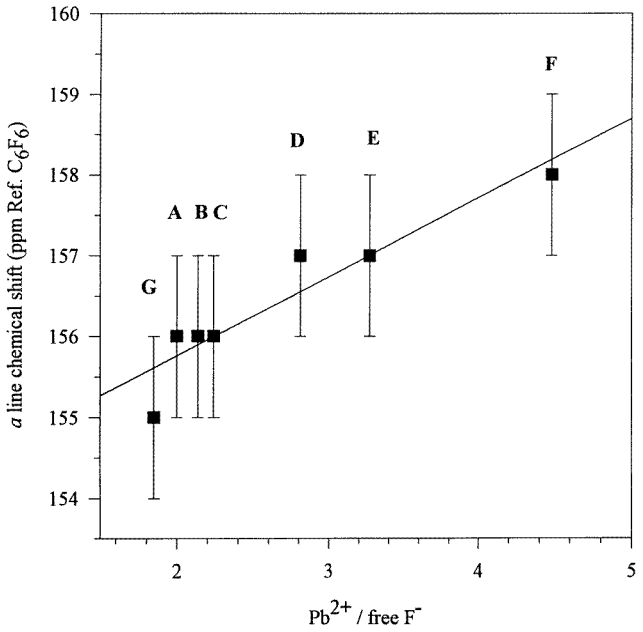

Figure 9. The chemical shift of the a line versus the mean number of Pb^{2+} ions for each free F^- ion.

4.4.2. Chemical shift variations. For the free fluorines, the variations of the chemical shift are plotted versus the ratio of Pb^{2+} ions to free fluorines in figure 9. They are quite small for the free fluorines, which confirms that the neighbourhood of these fluorines remains almost the same, as mentioned previously.

In figure 10, the variations of the chemical shift of the unshared fluorines are correlated with the ratio of Pb^{2+} ions to unshared fluorines in the glass. The chemical shift increase is directly proportional to this ratio, which indicates that the unshared-fluorine environment is strongly influenced by the Pb^{2+} ions. This result may be compared with the behaviour observed for the crystalline compounds: the greater the degree to which a F^- ion has Pb^{2+} ions in its neighbourhood, the higher the chemical shift.

In contrast, a natural correlation should be made between the Zn^{2+} ratio and the chemical shift of the shared fluorines. This may be understood if we assume that their neighbourhood involves essentially fluorines and two transition metal ions. This is why in figure 11 we plotted the chemical shift as a function of the proportion of ZnF_2. We can then verify that the behaviour is in accordance with the observation for the crystalline compounds. The greater the involvement of Zn^{2+} in this fluorine neighbourhood, the more the corresponding

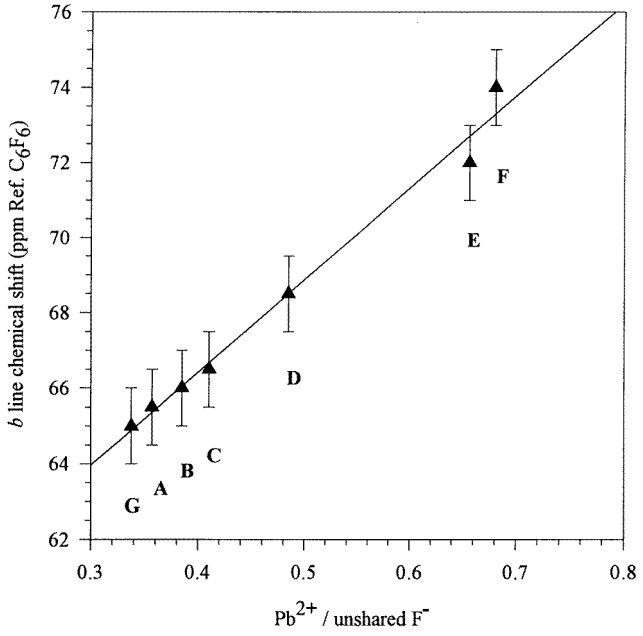

Figure 10. The chemical shift of the b line versus the mean number of Pb^{2+} ions for each unshared F^- ion.

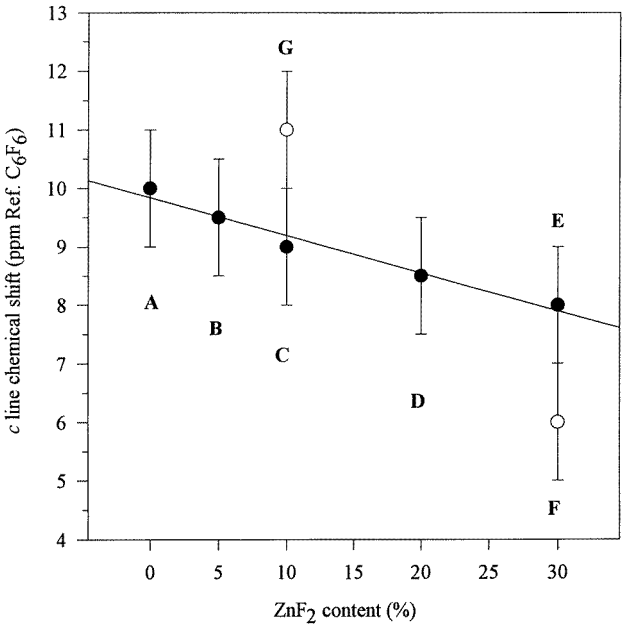

Figure 11. The chemical shift of the c line versus the ZnF_2 content in the starting melt.

NMR line is shifted towards the low values of the chemical shift, as previously shown in $CsZnGaF_6$. The apparent discrepancy observed for the G and F glasses may be correlated

with the variation of the proportion of PbF_2 (figure 3). The increase of the number of Pb^{2+} ions in PZG G glass induces a larger ^{19}F chemical shift. The opposite reasoning explains the lower value obtained for PZG F glass.

Note that in figures 8, 9, 10, and 11, the straight lines are the results of least-squares fits.

4.4.3. Chemical shift anisotropy. The values which are collected together in table 5 have been obtained through simulations of the experimental spectra which do not take into account the dipolar broadening explicitly. So, no definite conclusions could be drawn from these values. However, the confidence in the line intensity is not affected by this kind of reconstruction.

5. Conclusions

High-resolution solid-state MAS NMR experiments on ^{19}F in transition metal fluoride glasses have shown that the ^{19}F neighbourhood is quite different from the corresponding ones in the starting materials. Furthermore, we have demonstrated that the study of crystalline phases of close composition is very helpful for characterizing the ^{19}F environments. Thus, we have given clear evidence for three different kinds of fluorine environment in the PZG glasses. Furthermore, we were able to determine the ratios of the so-called free, shared, and unshared fluorines quantitatively from our NMR experiments on PZG glasses of various compositions. Owing to the direct free-fluorine ratio measurement, our results prove the validity of the previously adopted assumption according to which the glass network is built up from corner-sharing fluorine octahedra centred on transition metal ions. Through the determination of the mean number of fluorines per octahedron, we were able to show that the degree of cross-linking of these octahedra is strongly dependent on the glass composition, and may be varied from nearly 1D to nearly 3D connected octahedra. For instance, from our results, it may be inferred that the usual composition of PZG glass generally used in optical applications corresponds to PZG E, with a mean number of shared fluorines per octahedron of about 5, which is intermediate between the values for 2D and 3D connected octahedra.

References

[1] Dupas C, Le Dang K, Renard J P, Veillet P, Miranday J P and Jacoboni C 1981 *J. Physique* **42** 1345
[2] Lebail A, Jacoboni C and De Pape R 1985 *Mater. Sci. Forum* **6** 441
[3] Boulard B, Jacoboni C and Rousseau M 1989 *J. Solid State Chem.* **80** 17
[4] Lebail A, Jacoboni C and De Pape R 1983 *J. Solid. State Chem.* **48** 168
[5] Lebail A, Jacoboni C and De Pape R 1985 *J. Physique Coll.* **46** C8 163
[6] Legein C, Buzaré J Y, Emery J and Jacoboni C 1995 *J. Phys.: Condens. Matter* **7** 3853
[7] Legein C, Buzaré J Y, Boulard B and Jacoboni C 1995 *J. Phys.: Condens. Matter* **7** 4829
[8] Legein C, Buzaré J Y and Jacoboni C 1996 *J. Solid State Chem.* **121** 149
[9] Legein C, Buzaré J Y, Silly G and Jacoboni C 1996 *J. Phys.: Condens. Matter* **8** 4339
[10] Bobe J M, Senegas J, Réau J M and Poulain M 1993 *J. Non-Cryst. Solids* **162** 169
[11] Senegas J, Bobe J M and Réau J M 1994 *Solid State Commun.* **89** 983
[12] Bobe J M, Réau J M, Senegas J and Poulain M 1995 *Solid State Ion.* **82** 39
[13] Wang F and Grey C P 1995 *J. Am. Chem. Soc.* **117** 6637
[14] Boldrini P and Loopstsa B O 1967 *Acta Crystallogr.* **22** 744
[15] Wyckoff R W G 1965 *Crystal Structures* vol 1 (New York: Interscience)
[16] Brewer F M, Garton G and Goodgame D M L 1959 *J. Inorg. Nucl. Chem.* **9** 56
[17] Stacey L M, Vaughan R W and Elleman D D 1971 *Phys. Rev. Lett.* **26** 1153

[18] Lebail A, Jacoboni C and De Pape R 1986 *J. Solid State Chem.* **61** 188
[19] Samouël M and Champetier G 1969 *C. R. Acad. Sci., Paris* **268** 409
[20] Von Schnering H G 1967 *Z. Anorg. Allg. Chem.* **353** 13
[21] Jacoboni C, Le Bail A, De Pape R and Renard J P 1983 *J. Solid State Chem.* **3** 687
[22] Grannec J and Ravez J 1970 *Bull. Soc. Chim. Fr.* **5** 1753
[23] Von Der Muhll R, Andersson S and Galy J 1971 *Acta Crystallogr.* **27** 2345
[24] Boulard B 1989 *Thèse de l'Université du Maine* 89 LEMA 1001
[25] Eicher S M and Greedan J E 1984 *J. Solid State Chem.* **52** 12
[26] Perrot O 1994 *Thèse de l'Université du Maine* 94 LEMA 1008
[27] Massiot D, Thiele H and Germanus A 1994 *Bruker Rep.* **43** 140